From California's Extreme Drought to Major Flooding

Evaluating and Synthesizing Experimental Seasonal and Subseasonal Forecasts of Landfalling Atmospheric Rivers and Extreme Precipitation during Winter 2022/23

Michael J. DeFlorio, Agniv Sengupta, Christopher M. Castellano, Jiabao Wang,
Zhenhai Zhang, Alexander Gershunov, Kristen Guirguis, Rosa Luna Niño,
Rachel E. S. Clemesha, Ming Pan, Mu Xiao, Brian Kawzenuk, Peter B. Gibson,
William Scheftic, Patrick D. Broxton, Matthew B. Switanek, Jing Yuan,
Michael D. Dettinger, Chad W. Hecht, Daniel R. Cayan, Bruce D. Cornuelle,
Arthur J. Miller, Julie Kalansky, Luca Delle Monache, F. Martin Ralph,
Duane E. Waliser, Andrew W. Robertson, Xubin Zeng, David G. DeWitt,
Jeanine Jones, and Michael L. Anderson

KEYWORDS:
Atmospheric river;
Precipitation;
Seasonal
forecasting;
Seasonal variability;
Subseasonal
variability;
Water resources

ABSTRACT: California experienced a historic run of nine consecutive landfalling atmospheric rivers (ARs) in three weeks' time during winter 2022/23. Following three years of drought from 2020 to 2022, intense landfalling ARs across California in December 2022–January 2023 were responsible for bringing reservoirs back to historical averages and producing damaging floods and debris flows. In recent years, the Center for Western Weather and Water Extremes and collaborating institutions have developed and routinely provided to end users peer-reviewed experimental seasonal (1–6 month lead time) and subseasonal (2–6 week lead time) prediction tools for western U.S. ARs, circulation regimes, and precipitation. Here, we evaluate the performance of experimental seasonal precipitation forecasts for winter 2022/23, along with experimental subseasonal AR activity and circulation forecasts during the December 2022 regime shift from dry conditions to persistent troughing and record AR-driven wetness over the western United States. Experimental seasonal precipitation forecasts were too dry across Southern California (likely due to their over-reliance on La Niña), and the observed above-normal precipitation across Northern and Central California was underpredicted. However, experimental subseasonal forecasts skillfully captured the regime shift from dry to wet conditions in late December 2022 at 2–3 week lead time. During this time, an active MJO shift from phases 4 and 5 to 6 and 7 occurred, which historically tilts the odds toward increased AR activity over California. New experimental seasonal and subseasonal synthesis forecast products, designed to aggregate information across institutions and methods, are introduced in the context of this historic winter to provide situational awareness guidance to western U.S. water managers.

AFFILIATIONS: DeFlorio, Sengupta, Castellano, Wang, Zhang, Gershunov, Guirguis, Luna Niño, Clemesha, Pan, Xiao, Kawzenuk, Dettinger, Hecht, Kalansky, Delle Monache, and Ralph—Center for Western Weather and Water Extremes, Scripps Institution of Oceanography, University of California, San Diego, La Jolla, California; Gibson—National Institute of Water and Atmospheric Research, Wellington, New Zealand; Scheftic and Zeng—Department of Hydrology and Atmospheric Sciences, The University of Arizona, Tucson, Arizona; Broxton—School of Natural Resources and the Environment, The University of Arizona, Tucson, Arizona; Switanek—Department of Geography and Regional Science, University of Graz, Graz, Austria; Yuan and Robertson—International Research Institute for Climate and Society, Columbia University, Palisades, New York; Cayan, Cornuelle, and Miller—Division of Climate, Atmospheric Sciences, and Physical Oceanography, Scripps Institution of Oceanography, University of California, San Diego, La Jolla, California; Waliser—Jet Propulsion Laboratory, California Institute of Technology, Pasadena, California; DeWitt—Climate Prediction Center, NOAA/NWS/NCEP, College Park, Maryland; Jones and Anderson—California Department of Water Resources, Sacramento, California
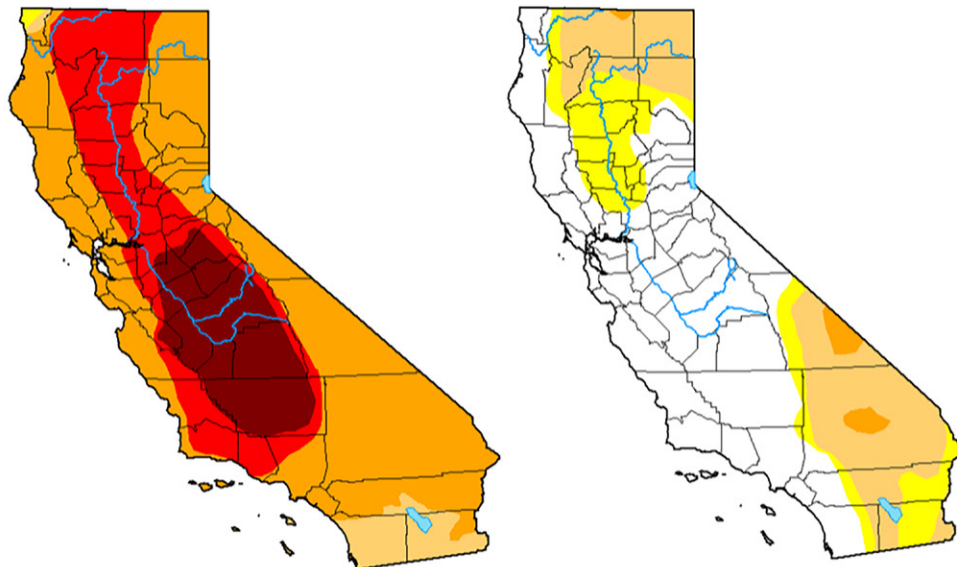
California entered the winter of 2022/23 with statewide emergency drought regulations in place and with water reservoirs at historically low levels, having endured several years of prolonged extreme and exceptional drought across much of the state (Guirguis et al. 2022; Krishnakumar and Kannan 2020). However, a family of nine atmospheric rivers (ARs) (Fish et al. 2019) and their associated extreme precipitation across California in late December 2022 and early January 2023 alleviated extreme and exceptional drought conditions across much of the state, while also causing an estimated $5–$7 billion in economic losses due to devastating floods, damaging winds, and debris flows (Moody's RMS 2023). Figure 1 shows U.S. Drought Monitor conditions across California at the start of the extended boreal winter season (issued: 27 September 2022) and at the end of the extended boreal winter season (issued: 28 March 2023). At the start of the water year, 94% of California was experiencing at least severe drought conditions according to the U.S. Drought Monitor, and 41% of California was experiencing extreme or exceptional drought. By the end of this remarkable winter (U.S. Drought Monitor, 28 March 2023), less than 10% of the state of California was experiencing severe drought conditions, and the extreme and exceptional drought that had evolved over years prior had been eliminated. As shown in Fig. 2, the Tulare basin six-station precipitation index cumulative precipitation was the highest in the 101 yr (1922–2023) period of record as of early April 2023 (50.6 in. or 128.5 cm from October 2022 to April 2023; 212% of average relative to 1991–2020), while the northern Sierra eight-station precipitation index cumulative precipitation totals were 133% of average over the same period (59.6 in. or 151.4 cm) according to data from the California Data Exchange Center (2023).

Unsurprisingly, the driver of the regional whiplash from historic drought to substantial rainfall during this period was a family of impactful ARs, which are lower-tropospheric jets of substantial water vapor transport that are responsible for nearly half of California's annual precipitation and streamflow (Gershunov et al. 2017; Dettinger et al. 2011; Ralph et al. 2004; Zhu and Newell 1998). Of primary importance in provoking this transition was a remarkable shift in the North Pacific–western North America atmospheric circulation regime from a high pressure ridge to a low pressure trough along the California coast that persisted throughout the 3 week period spanning from 26 December 2022 to 17 January 2023. Within this short span, nine ARs made landfall along the California coastline (Fig. 3). According to the AR scale ranking system introduced by Ralph et al. (2019), four of the ARs

California Drought Conditions: Late September 2022 vs. Late March 2023

Fig. 1. U.S. Drought Monitor conditions over California, issued by the National Drought Mitigation Center, on (left) 27 Sep 2022 and (right) 28 Mar 2023. Color shading represents drought intensity categories for abnormally dry (yellow), moderate drought (beige), severe drought (orange), extreme drought (red), and exceptional drought (maroon) conditions.

were moderate (AR2 ranking; maximum IVT = 500–750 kg m^{-1} s^{-1}; 1, 7, 14, and 16 January), four ARs were strong (AR3 ranking; maximum IVT = 750–1,000 kg m^{-1} s^{-1}; 31 December, and 5, 9, and 12 January), and one AR was exceptional (AR5 ranking; maximum IVT > 1,250 kg m^{-1} s^{-1}; 27 December).

Figure 4 provides another perspective of this shift over California from predominantly dry conditions during October 2022–November 2022 into AR-driven wet conditions during

Tulare Basin and Northern Sierra Cumulative Precipitation: October 2022 – April 2023 and Historical Context
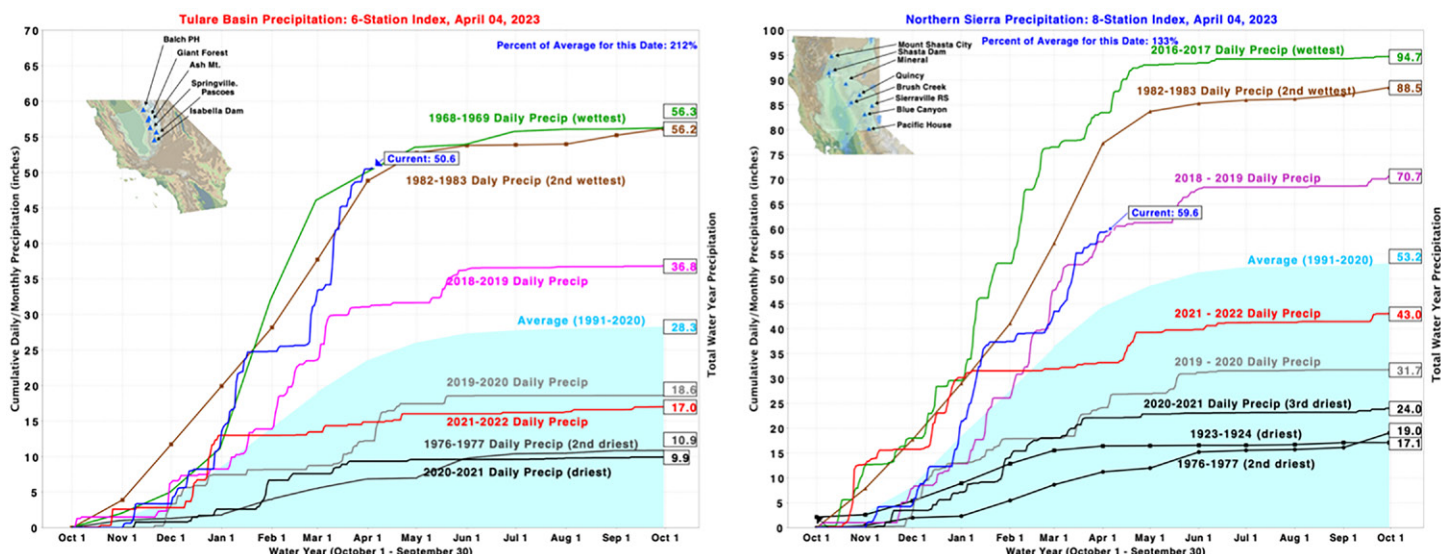

Fig. 2. (left) Tulare basin six-station precipitation index and (right) northern Sierra eight-station precipitation index for the 1 Oct 2022–4 Apr 2023 period. Cumulative precipitation in inches (*y* axis; 1 in. = 2.54 cm) is plotted as a function of date (*x* axis) for the current water year (dark blue line) and for a variety of historical water years (other colored lines).

Drought-Mitigating California AR Landfalls: December 26, 2022 – January 17, 2023
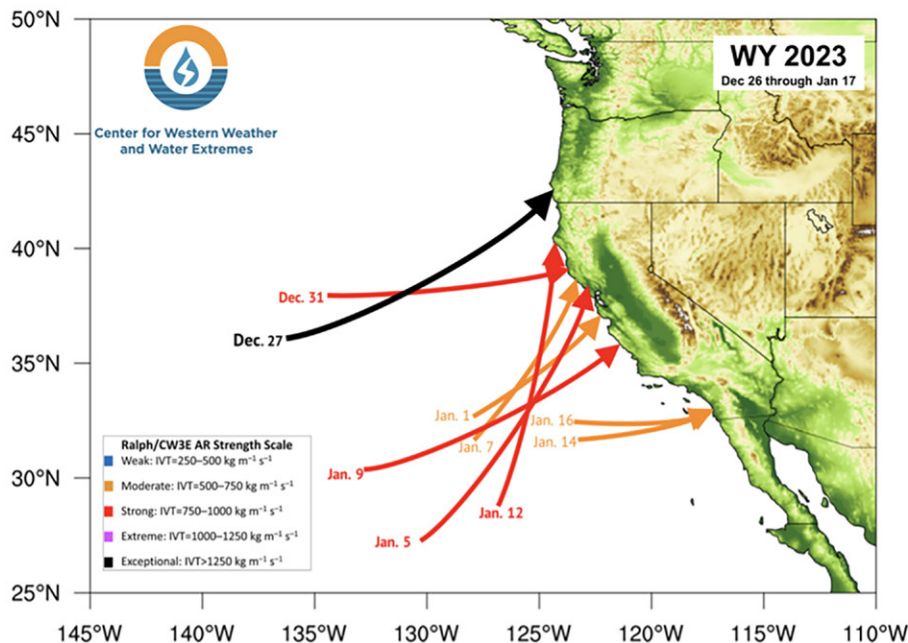

Fig. 3. Dates, landfall locations, directions, and strengths of nine atmospheric rivers (ARs) that made landfall along the California coastline from the 26 Dec 2022–17 Jan 2023 period. AR strength for each event is characterized using the AR scale ranking system introduced by Ralph et al. (2019).

December 2022–January 2023. Figure 4a shows daily mean coastal IVT associated with landfalling AR events according to the SIO-R1 AR catalog (Gershunov et al. 2017) from 1 October 2022 through 31 January 2023, and Fig. 4b shows daily zonal mean precipitation over California during this same period. The accumulated zonal mean precipitation over California for this period is shown in Fig. 4c. At all latitudes along the California coastline, zonal mean precipitation that fell during the October 2022–January 2023 period was above normal, with some areas receiving triple the amount of precipitation relative to average conditions (e.g., near 37°–38°N). Figures 4a and 4b visually convey the clustering of the ARs and their associated extreme precipitation during the late December 2022–early January 2023 period that substantially contributed to the total precipitation that fell during the broader period.

This remarkable family of landfalling ARs caused both benefits (e.g., reservoir replenishment) and hazards (e.g., flooding, high winds, and debris flows) and contributed a significant fraction of the total winter drought reduction across California. Figure 5 demonstrates this by showing deviations from the 1981–2010 normal of precipitation accumulated during October 2019 (beginning of recent drought) through November 2022 (Fig. 5a), total precipitation between December 2022 and January 2023 (Fig. 5b), and between October 2019 and January 2023 (Fig. 5c), with missing or extra overall precipitation expressed in terms of normal water years. During the October 2019–November 2022 period when drought was still widespread, the equivalent of 1–2 normal water years' worth of precipitation did not fall across much of Northern and Central California; Southern California was also in a precipitation deficit, but its magnitude was generally smaller (values between 0 and 1 normal water years equivalent deficit over much of coastal Southern California, with higher values between 1 and 2 near Santa Barbara County and over the Mojave Desert). However, by the end of the January 2023 season, many parts of Central California (including the Sierra range), as well as coastal Southern California, were no longer in deficit mode, as indicated by the white regions in Fig. 5c. Conditions improved dramatically across Northern California, though many areas remain in deficit compared to normal conditions for the 3.5 yr period shown in Fig. 5c.

AR Activity and California Precipitation: October 2022 – January 2023

a) Daily mean coastal IVT by landfalling ARs
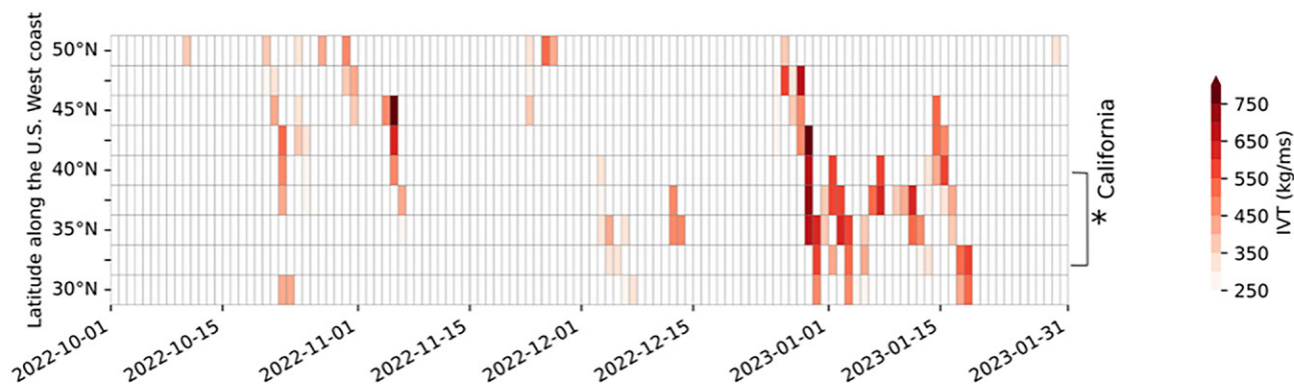
b) Daily zonal mean California precipitation
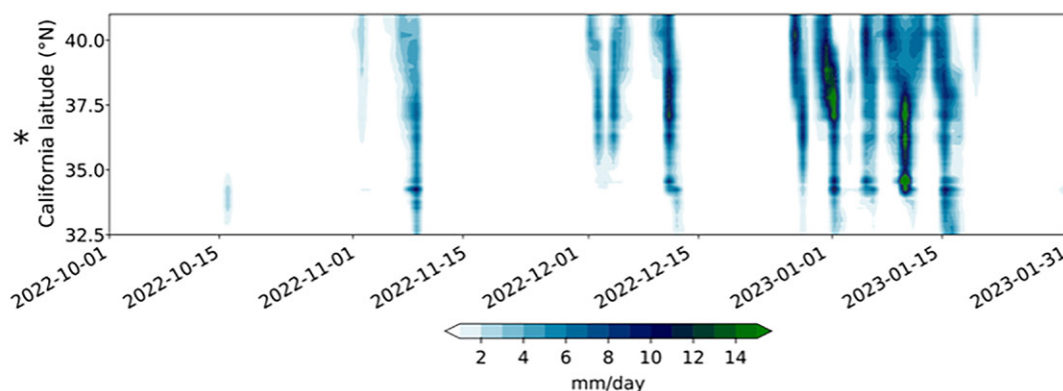
c) Total zonal precipitation (Oct-Jan)

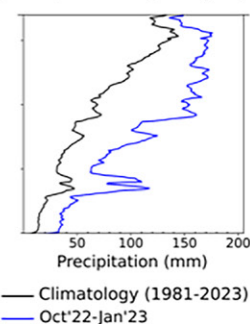**Fig. 4.** (a) Daily mean coastal integrated vapor transport (IVT) by AR events according to the SIO-R1 AR catalog (Gershunov et al. 2017); (b) daily zonal mean precipitation over California based on PRISM data (Daly et al. 2008); (c) total zonal mean California precipitation (blue line) through the October 2022–January 2023 period with comparison to climatology (black line; 1981–2023 period).

Notably, the inclusion of February 2023 and March 2023 in the calculation of Figs. 5b and 5c does not significantly modulate the magnitude and spatial structure of the "water years' worth of precipitation" metric evaluated in Fig. 5 (not shown).

California's transition from extreme multiyear drought to historic precipitation, flooding, and snowpack levels in just a few months' time made headlines around the world (e.g., Matza 2023; Toohey and Rust 2023), and prompted questions regarding the skill in various extended range prediction systems in forecasting this shift. This study will evaluate experimental seasonal and subseasonal prediction tools developed at the Center for Western Weather and Water Extremes (CW3E) (CW3E 2023), the NASA Jet Propulsion Laboratory (NASA JPL; in partnership with CW3E), The University of Arizona, the International Research Institute for Climate and Society (IRI) (IRI 2023), the NOAA Earth Systems Research Laboratory (NOAA ESRL), the North American Multimodel Ensemble (NMME), and the NOAA Climate Prediction Center (NOAA CPC) during the unprecedented 2022/23 winter over California. We also examine forecasts made for the upper Colorado River basin, an area whose water supply is of critical importance to over 40 million U.S. residents, including those located in many California communities. We will also introduce new experimental seasonal and subseasonal synthesis forecast products which assemble forecast information across these different institutions and methods. Emphasis will be placed on the December 2022 regime shift into AR-driven wet conditions, since this succession of storms was the first significant sign of drought alleviation across the state in several years. We note that the subsequent active AR

Water-Years Worth of Missing or Extra Precipitation: Before and After December 2022 – January 2023 Regime Shift into Strong AR Conditions
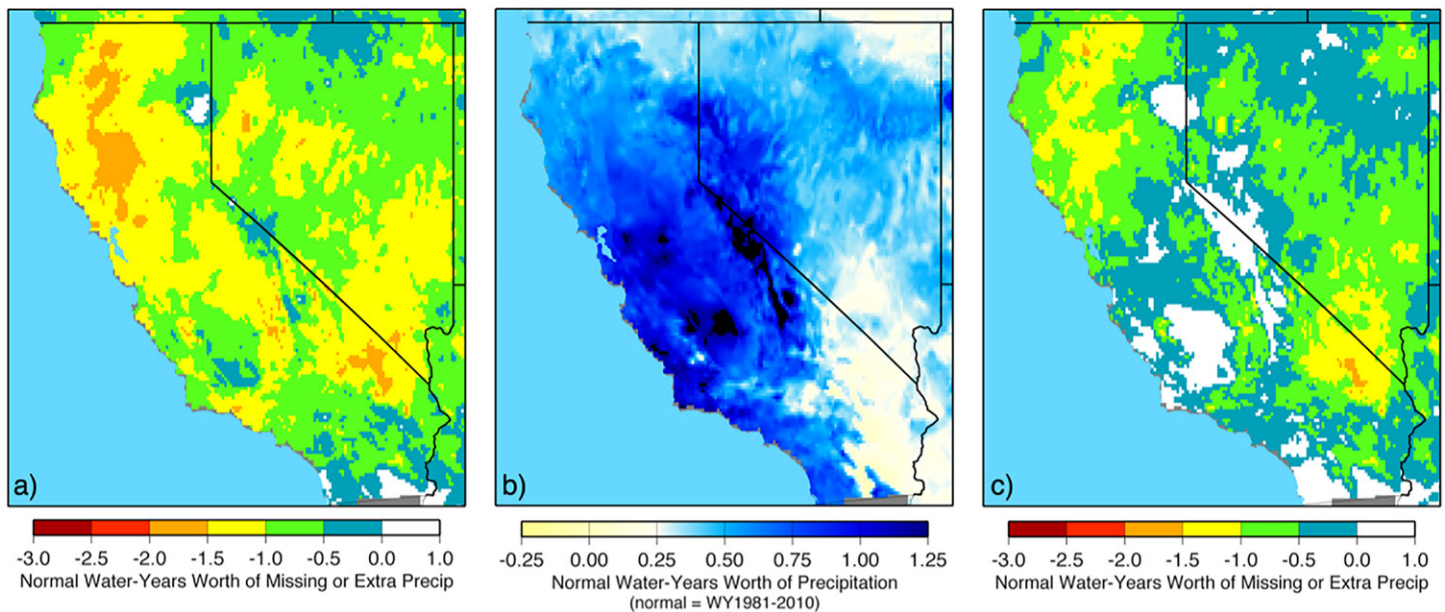
Fig. 5. Deviations from the 1981–2010 normal precipitation accumulated during (a) October 2019 (beginning of recent drought) through November 2022, (b) total precipitation between December 2022 and January 2023, and (c) between October 2019 and January 2023, with missing or extra overall precipitation expressed in terms of normal water years. White areas in (c) are regions where the net 3.5 years of precipitation anomalies were no longer in deficit mode by the end of January 2023. Precipitation amounts illustrated here are the PRISM 4-km-resolution monthly datasets.

and precipitation period in February 2023–March 2023 was also very important in continuing the replenishment of reservoirs and snowpack across the region. However, our evaluation focuses on the November 2022–January 2023 period, as it accounted for the statewide elimination of extreme and exceptional drought over California, and substantial reductions in the spatial extent of severe and moderate drought.

Experimental subseasonal and seasonal hydroclimate prediction tools generated at CW3E and collaborating institutions. Stakeholders and scientific organizations around the globe have increasingly recognized the need to improve prediction of total precipitation beyond weather time scales, as well as the drivers of hydroclimate variability, such as ARs and circulation regimes. End users stand to benefit from improvements in both subseasonal (2–6 week lead time) and seasonal (1–6 month lead time) forecasts of these variables (Gershunov and Cayan 2003; Waliser et al. 2006; Gottschalck et al. 2010; NASEM 2010, 2016; Vitart et al. 2017; Merryfield et al. 2020; Mariotti et al. 2020; DeFlorio et al. 2021; White et al. 2022; Sengupta et al. 2022). During this recent period of substantially increased investment in improving forecasts of hydroclimate variables beyond weather lead times, CW3E and collaborating institutions have investigated research topics and designed experimental forecast tools for ARs, circulation regimes, and total precipitation at both subseasonal (DeFlorio et al. 2019a,b; Gibson et al. 2020a,b; Robertson et al. 2020; Castellano et al. 2023; Wang et al. 2023; Zhang et al. 2023) and seasonal (Gershunov and Cayan 2003; Gibson et al. 2021; Kirtman et al. 2014; Switanek and Hamill 2022; Scheftic et al. 2023) lead times. In response to this growing suite of institutions, methods, and experimental forecast products, CW3E has recently created several new experimental subseasonal and seasonal synthesis forecast products to help summarize key experimental forecast information to stakeholders and end users (https://cw3e.ucsd.edu/s2s_forecasts/). In this paper, we will introduce these new experimental subseasonal and seasonal synthesis forecast

products, applied to the historic 2022/23 winter period over California and the upper Colorado River basin. In addition, the experimental forecasts from contributing universities, institutions, and agencies that populate the experimental synthesis products will be provided for context.

Synthesizing experimental seasonal precipitation forecasts during winter 2022/23
Overview of methods, regions of interest, and experimental seasonal forecasting terms.
At the start of water year 2023, experimental seasonal forecasts of precipitation were issued by several universities, institutions, and agencies across the United States. Despite important differences in underlying methodologies, each of these products provided probabilistic forecasts of precipitation across the western U.S. region. Figure 6 summarizes these forecasts for three key regions of interest to western U.S. water managers: Northern California, Southern California, and the upper Colorado River basin. The left panel shows the probabilistic forecasts in each region from each underlying method; the probabilistic category for the forecasts is denoted by symbols [above normal (+), below normal (−), normal (⊘), and uncertain/equal chances (U)], and the colors of the symbols correspond to individual universities, institutions, or agencies that issued the forecast. The uncertain/equal-chances category is issued for a forecast when a majority of ensemble members for a given prediction system disagree on the sign of the forecasted precipitation anomaly over the region of interest.

The right panel of Fig. 6 provides a tabular summary of the underlying methods, forecast period (five methods provide forecasts for November 2022–January 2023 and one for November 2022–March 2023), organizations, and regional summaries. Displaying the various probabilistic experimental seasonal precipitation forecasts in this collective and synthesized fashion enables easier end user interpretation of similarities and differences across the various methods, organizations, and regions of interest. For reference, each of the individual

Synthesized Experimental Seasonal Precipitation Forecasts: Winter 2022 - 2023

Methods	Forecast Period	Organization(s)	Nor Cal	So Cal	Upper Colo
Machine Learning based Forecast (Gibson et al.)	Nov-Jan	Jet Propulsion Laboratory / Center for Western Weather and Water Extremes	U	U	U
CCA Seasonal Precipitation Forecast (Gershunov et al.)	Nov-Jan	Center for Western Weather and Water Extremes	−	−	⊘
Univ. of Arizona Hybrid Seasonal Forecast (Zeng et al.)	Nov-Jan	A	U	⊘	+
IRI/CPC Forecast (Robertson et al.)	Nov-Jan	IRI	⊘	⊘	⊘
NOAA ESRL Seasonal Forecast (Switanek et al.)	Nov-Mar	Earth System Research Laboratory	⊘	−	⊘
NMME Seasonal Forecast	Nov-Jan	NMME	U	−	+
NOAA CPC Operational Outlook	Nov-Jan	NOAA	U	−	U

Legend:
- ✚ Above Normal
- ▬ Below Normal
- ⊘ Normal
- U Uncertain/Equal Chances

Organizations:
- Center for Western Weather and Water Extremes (SCRIPPS INSTITUTION OF OCEANOGRAPHY AT UC SAN DIEGO)
- Jet Propulsion Laboratory (California Institute of Technology)
- IRI, A

Fig. 6. Experimental seasonal precipitation forecasts for winter 2022/23 (November–January and November–March) issued by various organizations, institutions, and universities. Results are summarized over three key regions of interest to western U.S. water resource managers: Northern California (Nor Cal), Southern California (So Cal), and the upper Colorado River basin (Upper Colo). The symbols +, −, ⊘, and U denote above-normal, below-normal, normal, and uncertain/equal-chances precipitation categories, respectively.

forecasts presented in Fig. 6 is included in the online supplementary material (Figs. S2–S8; https://doi.org/10.1175/BAMS-D-22-0208.2). Several key studies documenting the historical skill of these experimental seasonal prediction systems include Gibson et al. (2021) (CW3E machine learning models), Gershunov and Cayan (2003) (CW3E CCA model), Scheftic et al. (2023) (U. Arizona model), Switanek and Hamill (2022) (ESRL model), and both Becker et al. (2022) and Kirtman et al. (2014) (NMME). The IRI experimental seasonal forecast is made at https://iri.columbia.edu/our-expertise/climate/forecasts/seasonal-climate-forecasts/.

For comparison, raw precipitation values (mm; left panel) and the associated anomalies (%; right panel) relative to normal conditions (1991–2020 baseline period) during the 1 November 2022–31 January 2023 period are shown in Fig. 7, calculated using PRISM data (Daly et al. 2008).[1] While case studies like this are useful, we caution readers that single forecasts cannot be used to infer the historical skill (or lack thereof) of any seasonal prediction system.

[1] We note that although the Switanek and Hamill method predicted precipitation through 31 March 2023, the overall magnitude and spatial structure of the precipitation anomaly fields are very similar whether the end date of the period of consideration is 31 January or 31 March (see Fig. S1).

Forecast evaluation over Northern California, Southern California, and upper Colorado River basin regions. In general, the suite of experimental seasonal precipitation forecasting methods summarized in Fig. 6 struggled to capture the large-scale precipitation anomaly patterns that were observed during the period of verification. However, there are notable exceptions, which will be discussed below. Over Northern California, observed precipitation anomalies ranged from 110% to 300% of normal; however, the experimental seasonal prediction systems favored above-normal precipitation over this region. Four of the methods forecasted uncertain/equal chances, two methods forecasted normal, and one method forecasted below normal. However, several individual models that are components of the individual prediction systems favored wetter-than-normal conditions across much of this region (especially over the Sierras and near the Bay Area), including the CW3E XGBoost and neural network machine learning models (Fig. S2), as well as the NMME GFDL-SPEAR model (not shown).
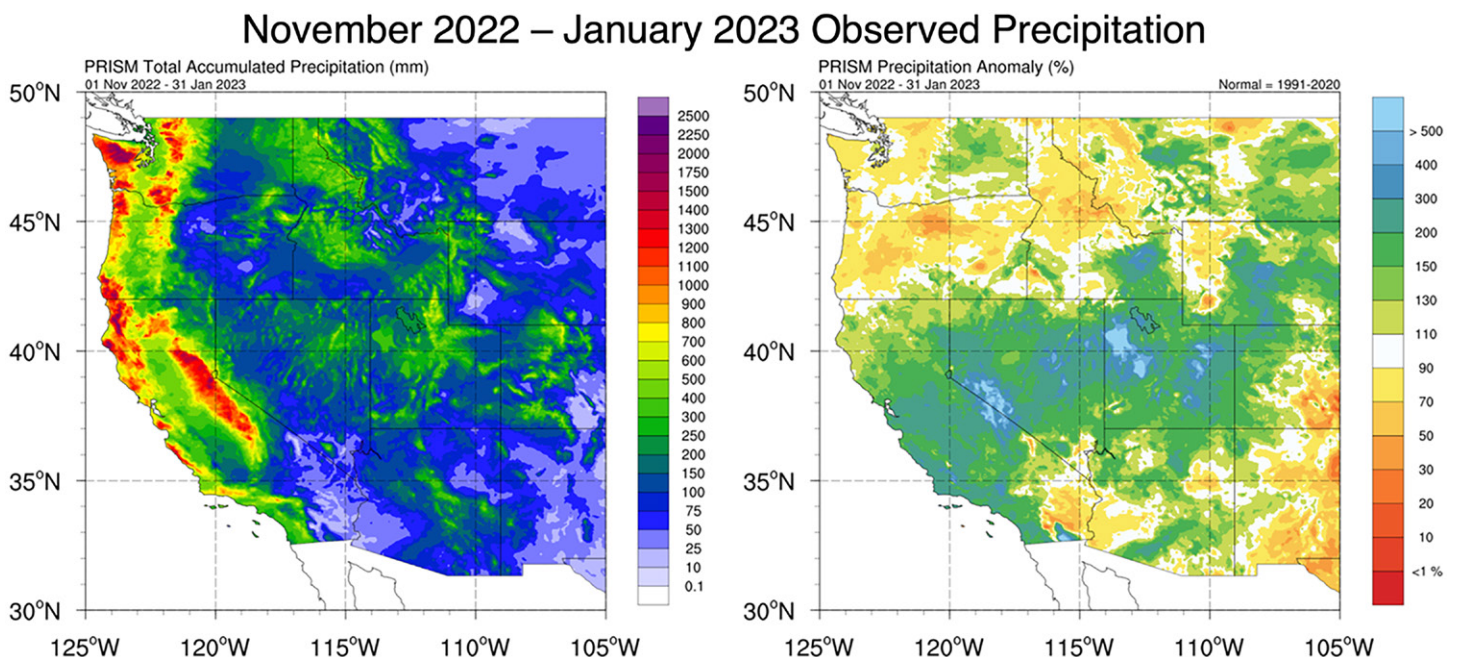

Fig. 7. Total raw accumulated (left) precipitation (mm) and (right) precipitation anomaly (%) for the 1 Nov 2022–31 Jan 2023 period. Anomalies in the right panel are calculated with respect to the 1991–2020 period. Precipitation data are obtained from the PRISM Climate Group (Daly et al. 2008).

Over Southern California, observed precipitation anomalies were generally above normal near coastal regions of Ventura, Los Angeles, Orange, and San Diego Counties, but were below normal over the eastern reaches of San Bernardino, Riverside, and Imperial Counties. A majority (four out of seven) of the experimental seasonal prediction systems forecasted below normal over Southern California (except for the IRI and University of Arizona forecasts, which were classified as normal, and the CW3E forecasts, which were classified as uncertain/equal chances). The prominence of below-normal precipitation forecasts over Southern California was not surprising, given that the phase and amplitude of El Niño–Southern Oscillation (ENSO) are generally among the most prominent predictor variables in all the prediction systems considered here, and that ENSO had remained in an extensive La Niña (cool) phase since 2020 (Fang et al. 2023). Additionally, drier-than-normal wintertime conditions over Southern California have been historically associated with the presence of preceding and contemporaneous La Niña events in the tropical Pacific (e.g., DeFlorio et al. 2013). Previous studies have examined similar seasonal precipitation forecasting busts over California during the winter of 2015/16, which was preceded by a strong El Niño event that did not bring predicted wetness to the state (Siler et al. 2017; Singh et al. 2018). It is also important to note that ENSO teleconnections related to North Pacific circulation anomalies are strongest in late winter compared to late fall and early winter (Chapman et al. 2021).

Across the upper Colorado River basin, observed precipitation anomalies were generally near normal or above normal, with some areas receiving up to ~400% of normal precipitation over the November–January period of interest (e.g., eastern Utah near the Colorado River and Green River confluence region). There was large uncertainty across methods in the precipitation anomaly category forecasts. Three methods forecasted normal conditions, and two methods each forecasted above normal or uncertain/equal chances.

Potential sources of error and future directions for western U.S. experimental seasonal precipitation forecasting. While significant progress has been made to date in designing, testing, and implementing innovative experimental seasonal prediction systems, the well-known challenges specific to seasonal forecasting of precipitation over California remain. These include the deficiency in dynamical models for predictions of ENSO-independent circulation anomalies at seasonal time scales over the North Pacific Ocean, and related Rossby wave train source regions (Jiang et al. 2022). In addition, many of the experimental seasonal prediction systems discussed in this study have been designed to predict total precipitation anomalies over the western U.S. region. However, as California experienced once again during winter 2022/23, ARs are often the driver of significant precipitation events during the winter season that disrupt ongoing periods of drought (Dettinger et al. 2011; Dettinger 2013; Ralph et al. 2018). Consequently, seasonal precipitation anomalies across California are highly sensitive to the occurrence of a handful of extreme events that can occur over a relatively short period. This was observed during the 26 December 2022–17 January 2023 period (only 23 days), during which much of Central California and Southern California received >50% of their normal total water year precipitation. Future experimental seasonal prediction systems that include ARs, AR-related precipitation, and integrated vapor transport (IVT) anomalies as predictands can be designed and compared against existing methods that are focused only on total precipitation.

Experimental subseasonal forecasts: Applications to December 2022–January 2023 active AR period over California and introduction of new CW3E experimental subseasonal synthesis forecast product

In the "Synthesizing experimental seasonal precipitation forecasts during winter 2022/23" section, we examined a wide range of experimental seasonal precipitation forecasts made at

the start of the 2022/23 winter season and introduced a new experimental seasonal synthesis forecasting product (shown in Fig. 6) to aid end users in interpreting and comparing experimental seasonal forecasts across different methods and research groups. In this section, we now shift our focus from seasonal forecasts toward subseasonal forecasts and the remarkable transition that occurred over the western United States from large-scale ridging and dry conditions to broad troughing that was associated with the landfall of nine ARs across the western U.S. coastline in a 3 week period from 26 December 2022 to 16 January 2023. We will examine the observed shift in circulation and IVT anomaly patterns over this period, along with the evolution of the Madden–Julian oscillation (MJO). Subsequently, we will evaluate experimental subseasonal forecasts of AR activity and circulation regimes made at CW3E and IRI. We will conclude this section by introducing a new experimental subseasonal synthesis forecast product developed at CW3E and in collaboration with stakeholders at the California Department of Water Resources (DWR).

Diagnosing the regime shift from widespread ridging and dry conditions to historic drought-mitigating AR activity over California. Figure 8 shows pentad mean precipitation (shading; mm day^{-1}), 500-hPa geopotential height anomalies (contours), and IVT (arrows; kg m^{-1} s^{-1}) during the 22 December 2022–30 January 2023 period. Into the third week of December, the western United States remained in a persistent ridging pattern, with positive Z500 anomalies (Z500a) covering much of the coastline, and widespread below-normal precipitation conditions persisting over land. However, during the last week of December, a

Evolution of North Pacific/Western U.S. Synoptic Conditions: late December 2022 – late January 2023
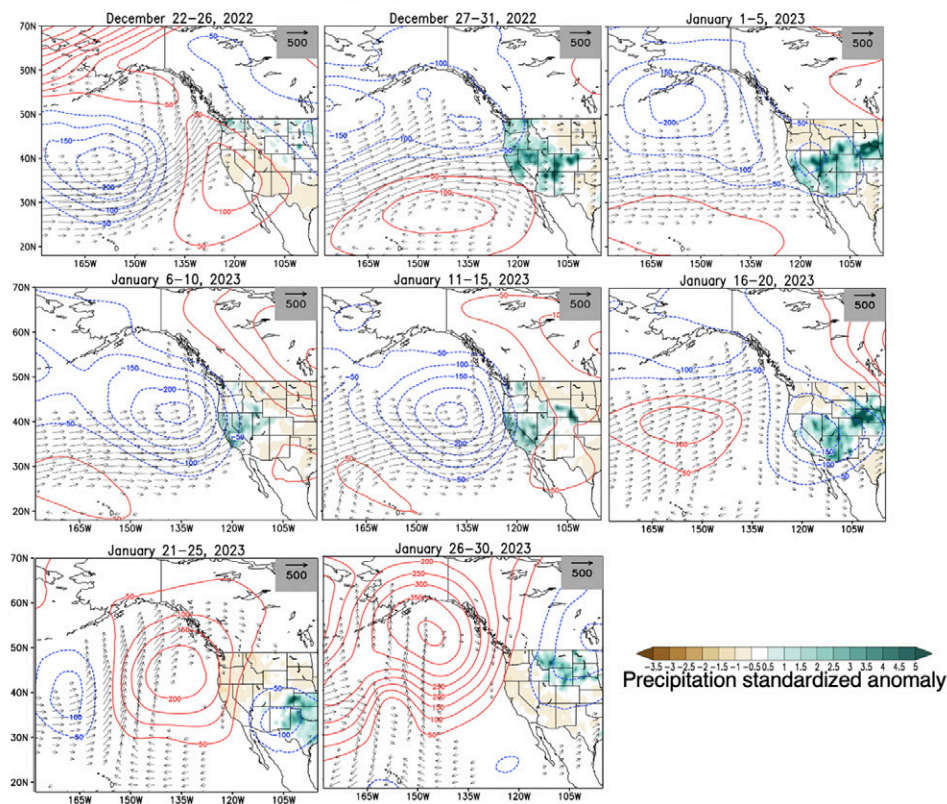
Fig. 8. Pentad mean precipitation (shading; mm day^{-1}), 500 hPa geopotential height anomalies (contours), and integrated vapor transport (arrows; kg m^{-1} s^{-1}) during the 22 Dec 2022–30 Jan 2023 period. Anomalies are calculated relative to the 1991–2020 climatology. Precipitation anomalies are standardized with green shading indicating positive anomalies and brown shading indicating negative anomalies. Red solid contours indicate positive geopotential height anomalies, and blue dashed contours indicate negative geopotential height anomalies. Geopotential height and IVT fields are obtained from ERA5 (Hersbach et al. 2020), and daily precipitation is obtained from NOAA CPC-Unified gauge-based analysis of daily precipitation over CONUS (Xie et al. 2007).

substantial change in the regional circulation occurred, with a shift to troughing conditions associated with substantial IVT anomalies directed at California's coastline. This regime of deep troughing, persistent AR activity, and associated above-normal precipitation conditions remained in place through the second week of January. During the 21–30 January period, ridging conditions centered over the Gulf of Alaska and offshore British Columbia regions emerged, marking the return of drier-than-normal conditions across the U.S. West Coast.

Observed evolution of the MJO during late December 2022–early January 2023. The MJO is a tropical planetary-scale convectively coupled system that has a period of approximately 30–60 days (Madden and Julian 1971, 1972). It travels from the Indian Ocean to the date line where its convective signal often tends to diminish. The diabatic heating associated with the MJO leads to the formation of an anomalous Rossby wave source in the subtropics, from which a Rossby wave propagates eastward along the jet and emanates at the exit region in the midlatitudes. As a result, these MJO teleconnections can strongly modulate midlatitude weather and climate phenomena, including precipitation and temperature patterns (Zhou et al. 2012), ARs (Mundhenk et al. 2016; Zhou et al. 2021), and storm tracks (Deng and Jiang 2011). MJO teleconnections evolve with the eastward MJO propagation in the tropics. When the MJO is active over the western Pacific Ocean, there is a higher likelihood of anomalous troughing occurring over the North Pacific. This would lead to anomalous eastward moisture transport over the subtropical Pacific Ocean and the U.S. West Coast, along with an increased chance of AR activity and extreme precipitation. When the MJO is active over the Indian Ocean, there is a higher likelihood of anomalous ridging over the North Pacific, and ultimately the likelihood of AR activity and extreme precipitation over the U.S. West Coast decreases (Guan et al. 2012; Guan and Waliser 2015; Mundhenk et al. 2018; Wang et al. 2023).

Given the relevance of the MJO in modulating western U.S. extreme precipitation, and its potential importance as a relevant predictor variable for subseasonal forecasting, we next examine the observed behavior of the MJO concurrent with the circulation regime shift from dry to wet conditions described in the previous section. Figure 9a shows the MJO phase diagram for the 14 December 2022–22 January 2023 period. During the 20–28 December 2022 period, the MJO was active over the Maritime Continent region (phases 4 and 5) and then propagated into the western Pacific (phases 6 and 7) during the 29 December 2022–5 January 2023 period.

Figure 9b shows the 5–9-day-averaged lagged response of MERRA2 filtered Z500 and IVT anomalies to day-0 MJO phases 4 and 5 and 6 and 7 during the November–January (NDJ) period composited over the 1980–2020 historical record. In the historical record, a transition of the MJO from phases 4 and 5 to phases 6 and 7 is associated with a weakening of Z500a along the western U.S. coastline and a circulation pattern that is more favorable for IVTa associated with ARs directed toward the California coastline. We more closely investigate the historical relationships of extreme precipitation anomalies and ARs themselves with these particular MJO phase combinations in Figs. 9c and 9d based on the results from Wang et al. (2023).

Figure 9c shows the 5–9-day-averaged lagged response of AR frequency in NDJ after MJO phases 4 and 5 and 6 and 7 composited over 1980–2020. Figure 9d shows absolute changes (defined as precipitation extremes in strong MJO phases minus climatology) in frequency (%) of wet extremes averaged over 5–9 lagged days after active MJO days in phases 4 and 5 and 6 and 7 (shading). The extremes were selected when the CPC daily precipitation over 1979–2019 exceeds the 95th percentile of the gamma distribution of nonzero precipitation.

The composites in Figs. 9c and 9d show that a phase shift of an active MJO event from phases 4 and 5 to phases 6 and 7 is consistent with tipping the odds in favor of higher frequency of ARs and extreme precipitation across much of California during NDJ. Although

Evolution of MJO Conditions: late December 2022 – early January 2023 and Historical Context
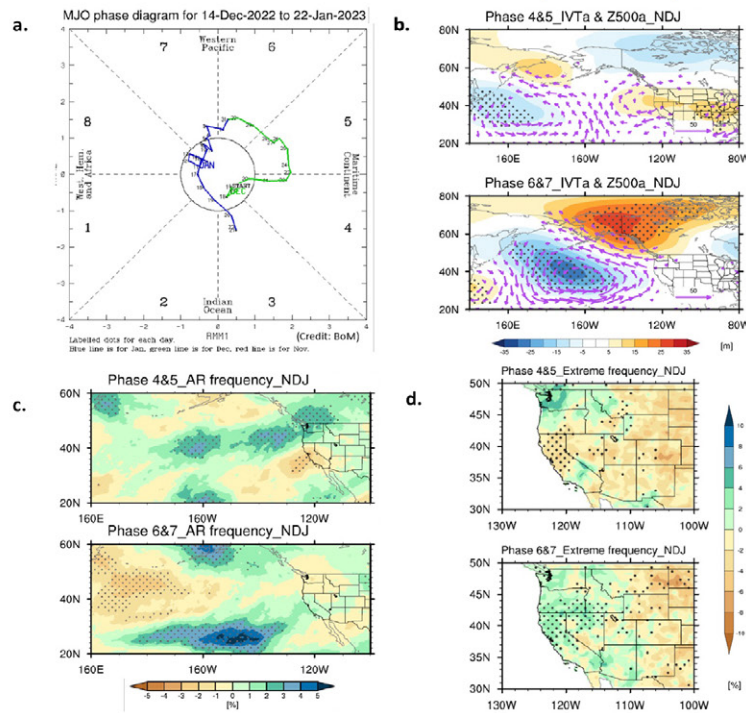
Fig. 9. (a) MJO phase diagram for the 14 Dec 2022–22 Jan 2023 period, provided by the Australian Bureau of Meteorology (BoM). The green line is for December 2022, and the blue line is for January 2023. (b) The 5–9-day-averaged lagged response of MERRA2 filtered Z500 (shading; m) and IVT (vectors; kg m^{-1} s^{-1}) anomalies to day 0 MJO phases 4 and 5 and 6 and 7 in November–January (NDJ) composited over 1980–2020. The dotted areas represent significant Z500 anomalies (Z500a) exceeding the 95% confidence level according to the two-tailed Student's t test. Vectors that are shown are significant IVT anomalies (IVTa). (c) The 5–9-day-averaged lagged response of AR frequency in NDJ after MJO phases 4 and 5 and 6 and 7 composited over 1980–2020. The AR frequency was determined based on the MERRA2 AR detection dataset (Guan and Waliser 2015; Guan et al. 2018). The stippled areas represent significant AR changes exceeding the 95% confidence level according to the 1,000-times-iteration moving-blocks bootstrapping test. (d) Absolute changes (defined as precipitation extremes in strong MJO phases minus climatology) in frequency (%) of wet extremes averaged over 5–9 lagged days after active MJO days in phases 4 and 5 and 6 and 7 (shading). The extremes were selected when the CPC daily precipitation over 1979–2019 exceeds the 95th percentile of the gamma distribution of nonzero precipitation. Dots indicate that the changes are significant relative to climatology over the 95% confidence level based on the bootstrap test.

many other processes within the climate system can destructively interfere with canonical MJO teleconnection patterns, we find here that the above-normal AR activity and the associated extreme precipitation over California during late December 2022 and early January 2023 are consistent in sign with (although larger in magnitude than) historical relationships between the MJO and western U.S. extreme precipitation frequency analyzed in Wang et al. (2023). Future studies examining the role of other modes of climate variability relevant to subseasonal and seasonal prediction [e.g., the Arctic Oscillation (AO) and ENSO] in potentially influencing the observed regime shift and increase in AR activity along the California coastline would be valuable to both the research community and stakeholders interested in this historic period. For example, changes in MJO characteristics may affect its resultant impact on extreme precipitation over the western U.S. region. Toride and Hakim (2022) found that western U.S. ARs tend to occur more often when the MJO is more stationary and propagates at a slower speed. The background state is also important. In addition, the MJO may lead to more western U.S. ARs during El Niño conditions (Toride and Hakim 2022).

Evaluation of experimental subseasonal weather regime (IRI) and AR activity (CW3E) forecast products. Figures 8 and 9 provide diagnostics of the observed circulation regime shift and accompanying phase transition of the MJO during late December 2022 and early

January 2023. We now shift our focus toward evaluating two experimental subseasonal forecast products during this period: the IRI experimental subseasonal weather regime outlook (Robertson et al. 2020), and the CW3E experimental subseasonal AR activity outlook (DeFlorio et al. 2019b).

Figure 10 shows the IRI experimental subseasonal weather regime outlook, based on CFSv2 forecasted large-scale circulation regimes (colors) versus lead time (*y* axis) for daily forecasts starting from 1 October 2022 to 23 January 2023 (*x* axis). This outlook was subsequently updated every day until 31 March 2023, filling in the entire plot. Color shading that is constant in the vertical direction corresponds to a regime pattern that was skillfully predicted at a lead time corresponding to the *y*-axis value where the shading changes color. The color saturation provides an estimate of the forecast probability, computed from the number of ensemble members closest to that regime centroid. The goal of this analysis was to identify and graphically depict the CFSv2 forecasts and their evolution in terms of large-scale circulation/teleconnection patterns as guidance for forecasters.

Throughout much of October 2022 and November 2022, the IRI outlook alternated between Pacific ridge (blue) and West Coast ridge (red) conditions, which are historically associated with widespread positive Z500 anomalies centered over the Gulf of Alaska and North American coastline, respectively, and accompanying below-normal precipitation anomalies over California (Robertson et al. 2020). We note that the historical relationship between below-normal precipitation anomalies over California is much stronger and more
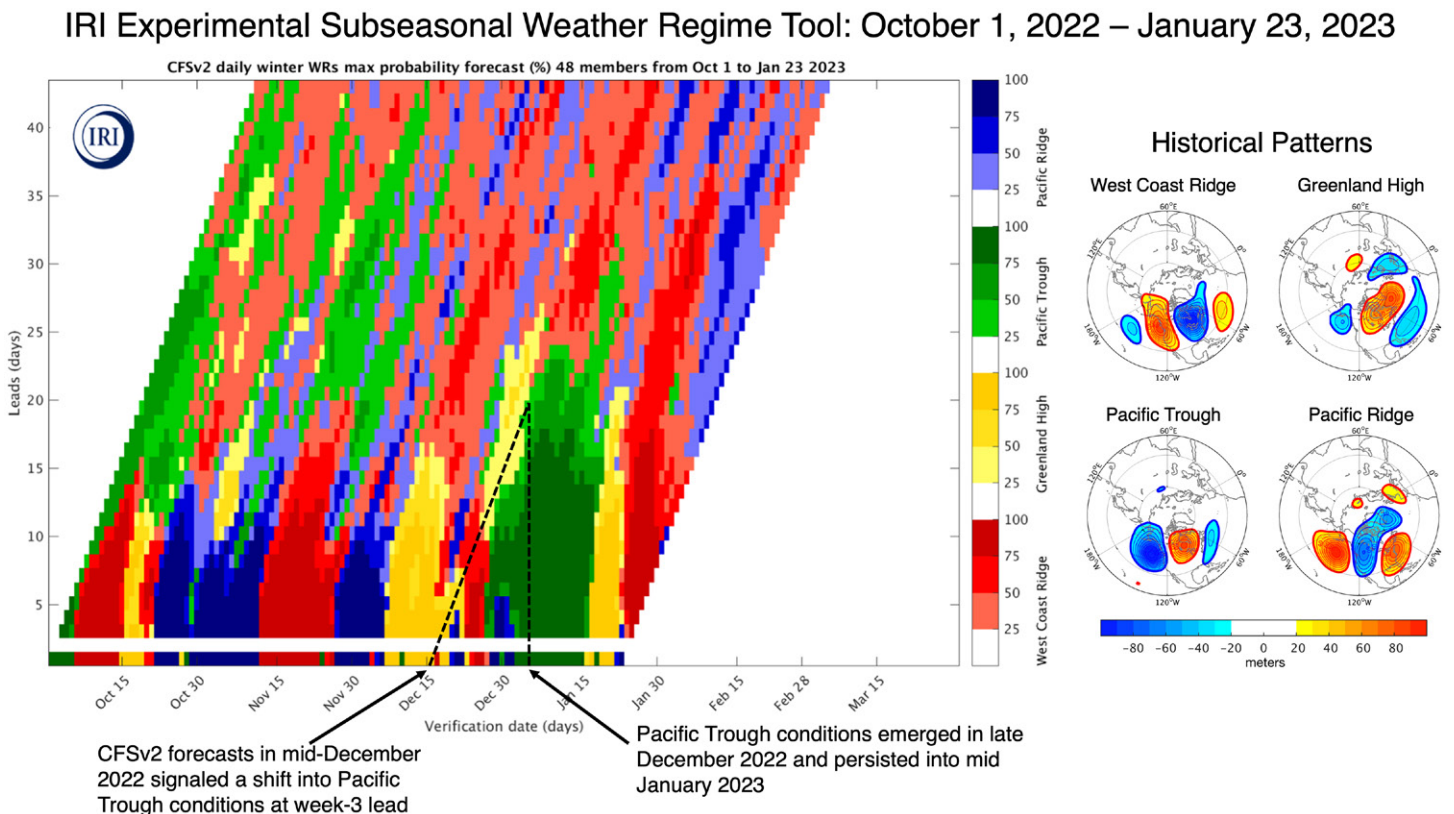
Fig. 10. (left) International Research Institute for Climate and Society (IRI) experimental subseasonal weather regime outlook, based on CFSv2 forecasted large-scale circulation regimes (colors) vs lead time (*y* axis) for daily forecasts starting from 1 Oct 2022 to 23 Jan 2023 (*x* axis). The forecasts were subsequently updated every day through 31 Mar 2023. Colors indicate the observed regime pattern (labeled on right) that the CFSv2 forecast most closely resembles (mean of 48 members of a 3-day lagged ensemble, smoothed with 5-day running averages), expressed as a percentage of ensemble members. Thus, the plotted sequence for a lead of 3 days represents an average over days 1–5 of the forecast, and lead of 2 days is left white. The daily evolution of the CFSv2 analysis (i.e., the lead-0 forecast) is shown along the bottom of the plot. Color saturation provides an estimate of the similarity between the observed historical regime pattern (from MERRA; introduced in Robertson et al. 2020) and the forecast ensemble mean. (right) The historical regime patterns are shown for reference.

spatially extensive during West Coast ridge conditions compared to Pacific ridge conditions. Throughout the first 2 weeks of December, the observed circulation regime most closely resembled the Greenland high (yellow) pattern, which is also associated with below-normal precipitation anomalies over Northern California (though the anomalies are not statistically significant). However, beginning around the second week of December, the IRI tool showed a forecasted shift into Pacific trough (green) conditions 2–3 weeks later during the end of December and early January. This predicted regime shift verified around 30 December 2022 and represents a skillful CFSv2 experimental subseasonal forecast for the observed transition from widespread ridging and associated dry conditions over California to deep troughing and successive landfalling ARs along the California coastline. We also note that this was a somewhat chaotic transition between 26 December 2022 and 2 January 2023, as all four regime types appeared before Pacific trough regime conditions finally stabilized into the third week of January.

This substantial regime shift in December 2022 from ridging to troughing conditions appears to have been more predictable than the regime transitions earlier in the water year. For example, during October–November, we see skill in certain regime shifts on the order of 10–15 days, whereas starting in late December we see more extensive skill in weeks 2–3. Understanding these skill differences is a topic for further research and is being explored in ongoing studies using methods introduced by Guirguis et al. (2020).

In addition, we note that while this December 2022 regime shift was generally well forecasted, the circulation regimes forecasted using this methodology represent large-scale patterns that do not always capture important details along the coast that might affect AR landfalls and precipitation over California. To gain a more detailed look at the forecasted impacts associated with this developing Pacific trough regime, we use the AR activity forecasts developed for weeks 1–4.

An evaluation of the CW3E experimental subseasonal AR activity outlook (DeFlorio et al. 2019b) during this period is shown in Fig. 11 for the week-3 lead time. Forecasts initialized at 0000 UTC 8 December 2022 (top row), 0000 UTC 22 December 2022 (middle row), and 0000 UTC 5 January 2023 (bottom row) forecasts (week-3 lead time) from the National Centers for Environmental Prediction (NCEP) (left column), Environment and Climate Change Canada (ECCC) (center-left column), and European Centre for Medium-Range Weather Forecasts (ECMWF) (center-right column) subseasonal dynamical ensembles, along with observed AR activity based on ERA5 data (right column). The valid period for each forecast is 23–29 December 2022 (top row), 6–12 January 2023 (middle row), and 20–26 January 2023 (bottom row). Values plotted are the ensemble mean forecast anomalies relative to each model's hindcast climatology (left three columns) and observed anomalies relative to the ERA5 climatology (right column). Consistent with the skillful weeks-2–3 lead-time regime shift discussed previously, the AR activity outlooks based on dynamical model data from each of the three centers showed significant AR activity over the North Pacific and western U.S. coastline for both the 23–29 December 2022 and 6–12 January 2023 valid periods. Although the models were not skillful in capturing finer-resolution details of these weekly AR activity periods (e.g., the extent of inland AR penetration), it is clear from an evaluation of these two experimental subseasonal forecast tools that they were able to capture the large-scale shift in regional circulation patterns and its associated increase in AR activity, leading to the historic drought-mitigating precipitation observed over California in the late December 2022–mid-January 2023 period. In addition, the week-3 forecasts in both the ECCC and ECMWF ensemble systems skillfully predicted the end of this active AR period and a temporary return to dry conditions observed from 20 to 26 January 2023, though the observed magnitude of below AR activity anomalies across the western United States was higher than predicted, and the NCEP model failed to predict this shift. We emphasize that despite

CW3E Experimental Subseasonal AR Activity Tool: Late December 2022 and Early January 2023 Week-3 Forecasts and Verification
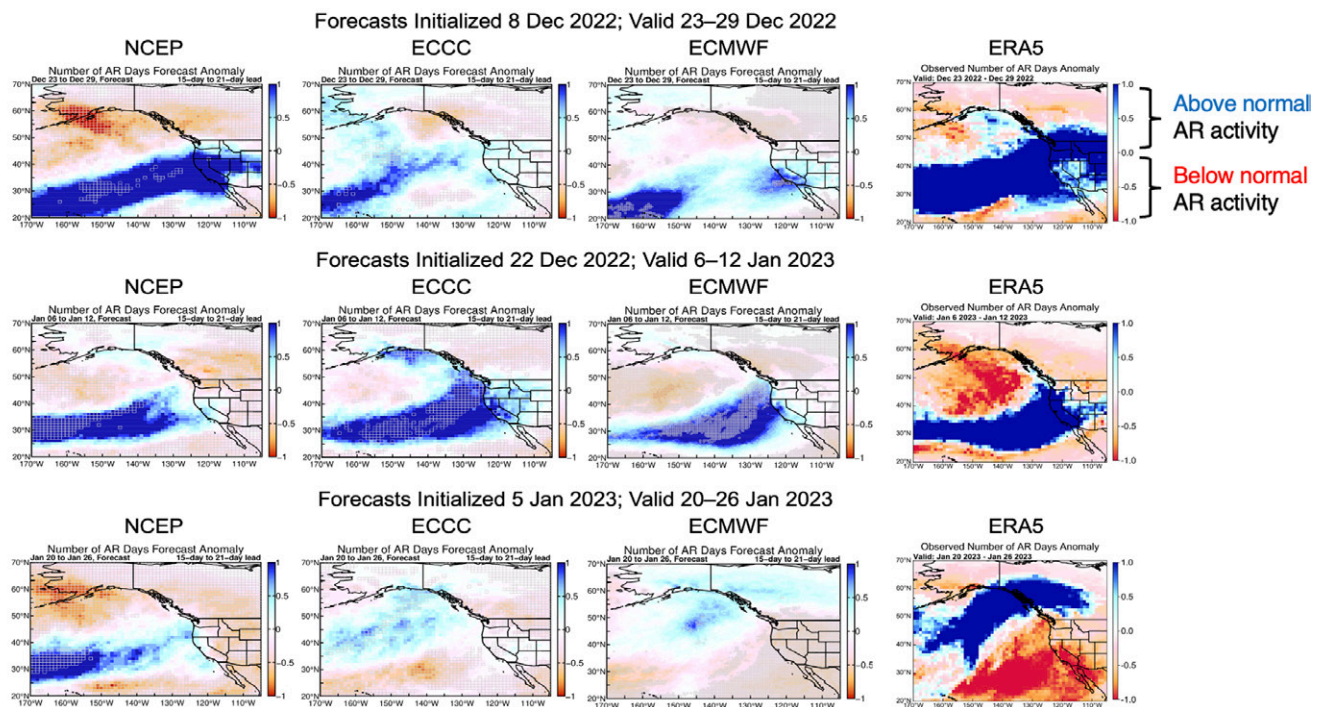

Fig. 11. Center for Western Weather and Water Extremes (CW3E) experimental subseasonal atmospheric river activity outlooks (introduced in DeFlorio et al. 2019b) for (top) 0000 UTC 8 Dec 2022, (middle) 0000 UTC 22 Dec 2022, and (bottom) 0000 UTC 5 Jan 2023 forecasts (week-3 lead time) from the (left) National Centers for Environmental Prediction (NCEP), (center left) Environment and Climate Change Canada (ECCC) and (center right) European Centre for Medium-Range Weather Forecasts (ECMWF) subseasonal dynamical ensembles, along with (right) observed AR activity based on ERA5. Values plotted are the ensemble-mean forecast anomalies relative to each model's hindcast climatology in the left three columns and observed anomalies relative to the ERA5 climatology in the right column. The valid period for each forecast is (top) 23–29 Dec 2022, (middle) 6–12 Jan 2023, and (bottom) 20–26 Jan 2023.
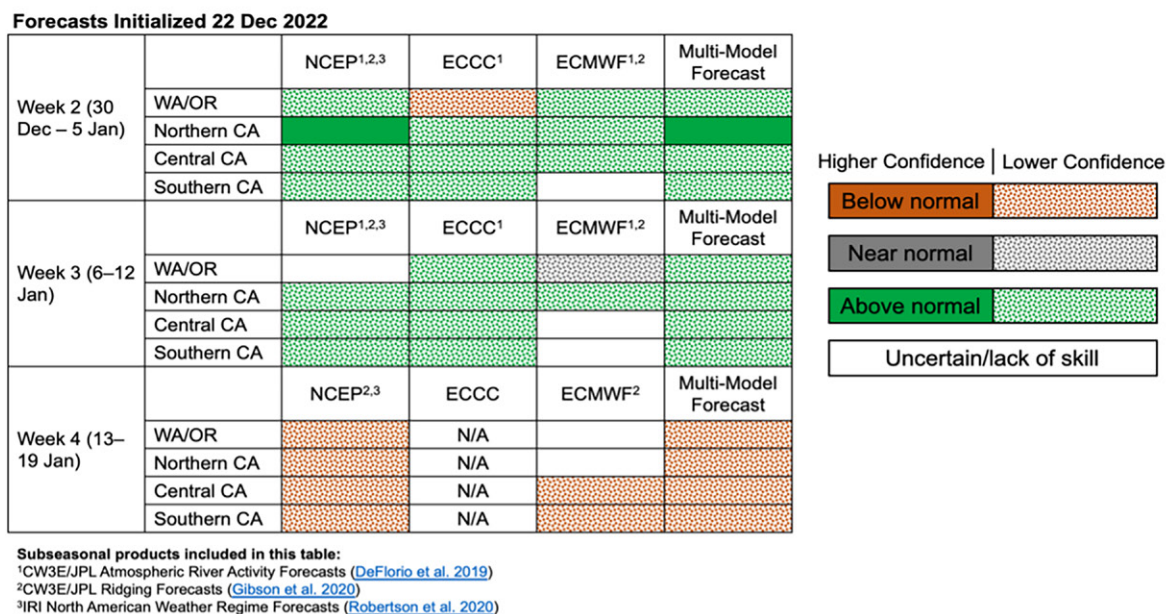
the relative skill in dynamical ensemble predictions of the regime shift investigated here, substantial barriers remain in generating reliable experimental subseasonal predictions of circulation regimes, ARs, and precipitation over the western United States for end users.

CW3E experimental subseasonal synthesis forecast product: 22 December 2022 forecast.
During the last two winters, CW3E researchers have worked in close coordination with collaborators to create experimental subseasonal synthesis forecast products that seek to provide probabilistic categories of precipitation anomalies summarized across three individual experimental subseasonal forecast products: the aforementioned CW3E experimental subseasonal AR activity outlooks (DeFlorio et al. 2019b) and IRI experimental subseasonal weather regime outlooks, as well as the CW3E experimental subseasonal ridging outlooks (Gibson et al. 2020a,b). These products were designed in tandem with stakeholders at the California DWR, who provided significant input and feedback to help improve the interpretability of the outlooks for end users.

An example of this forecast synthesis product is shown in Fig. 12 for the 0000 UTC 22 December 2022 dynamical model forecast alluded to previously. The regions summarized in the experimental subseasonal synthesis tool include Washington/Oregon (WA/OR), Northern California, Central California, and Southern California (each row). Forecast results from NCEP, ECCC, and ECMWF are shown, respectively, in each column. The superscripts indicate the different types of subseasonal products being considered in the synthesized forecasts. High confidence is determined when there is a ≥75% probability (fraction of ensemble members in

CW3E Experimental Subseasonal Synthesis Forecast Product: December 22, 2022 Forecasts

Forecasts Initialized 22 Dec 2022

Week 2 (30 Dec – 5 Jan)		NCEP[1,2,3]	ECCC[1]	ECMWF[1,2]	Multi-Model Forecast
	WA/OR	Above normal (lower conf.)	Below normal (lower conf.)	Above normal (lower conf.)	Above normal (lower conf.)
	Northern CA	Above normal (higher conf.)	Above normal (lower conf.)	Above normal (lower conf.)	Above normal (higher conf.)
	Central CA	Above normal (lower conf.)	Above normal (lower conf.)	Above normal (lower conf.)	Above normal (lower conf.)
	Southern CA	Above normal (lower conf.)	Above normal (lower conf.)	Uncertain/lack of skill	Above normal (lower conf.)

Week 3 (6–12 Jan)		NCEP[1,2,3]	ECCC[1]	ECMWF[1,2]	Multi-Model Forecast
	WA/OR		Above normal (lower conf.)	Near normal (lower conf.)	Above normal (lower conf.)
	Northern CA	Above normal (lower conf.)	Above normal (lower conf.)	Above normal (lower conf.)	Above normal (lower conf.)
	Central CA	Above normal (lower conf.)	Above normal (lower conf.)	Above normal (lower conf.)	Above normal (lower conf.)
	Southern CA	Above normal (lower conf.)	Above normal (lower conf.)	Above normal (lower conf.)	Above normal (lower conf.)

Week 4 (13–19 Jan)		NCEP[2,3]	ECCC	ECMWF[2]	Multi-Model Forecast
	WA/OR	Below normal (lower conf.)	N/A		Below normal (lower conf.)
	Northern CA	Below normal (lower conf.)	N/A		Below normal (lower conf.)
	Central CA	Below normal (lower conf.)	N/A	Below normal (lower conf.)	Below normal (lower conf.)
	Southern CA	Below normal (lower conf.)	N/A	Below normal (lower conf.)	Below normal (lower conf.)

Legend: Higher Confidence | Lower Confidence — Below normal; Near normal; Above normal; Uncertain/lack of skill

Subseasonal products included in this table:
[1]CW3E/JPL Atmospheric River Activity Forecasts (DeFlorio et al. 2019)
[2]CW3E/JPL Ridging Forecasts (Gibson et al. 2020)
[3]IRI North American Weather Regime Forecasts (Robertson et al. 2020)

Fig. 12. CW3E experimental subseasonal (weeks-2–4 lead time) synthesis forecast product for 0000 UTC 22 Dec 2022 subseasonal dynamical ensemble forecasts. The regions include Washington/Oregon (WA/OR), Northern California, Central California, and Southern California (each row). Forecast results from three models (NCEP, ECCC, ECMWF) are shown, respectively, in each column. The superscripts indicate the different types of subseasonal products being considered in the synthesized forecasts. High confidence is determined when there is a ≥75% probability of a pattern conducive to above-normal, below-normal, or near-normal conditions, and if the majority (>50%) of the forecast products agree on the sign of the anomaly. Low confidence is determined when there is a <75% probability of a pattern conducive to above-normal, below-normal, and near-normal conditions, and >50% of the forecast products agree on the sign of the anomaly. If the individual forecast products disagree on the sign of the anomaly, the synthesized forecast is classified as uncertain.

each model) of a pattern conducive to above-normal, below-normal, or near-normal conditions in an individual forecast project, and if the majority (>50%) of the forecast products agree on the sign of the anomaly. Low confidence is determined when there is a <75% probability of a pattern conducive to above-normal, below-normal, and near-normal conditions, and >50% of the forecast products agree on the sign of the anomaly. If the individual forecast products disagree on the sign of the anomaly, the synthesized forecast is classified as uncertain. For this example, the multimodel probabilistic forecast was for above-normal precipitation to occur in all four regions at both week-2 (30 December 2022–5 January 2023 valid period) and week-3 (6–12 January 2023 valid period) lead times, with the highest confidence over Northern California. The multimodel probabilistic forecast also favored a return to below-normal precipitation conditions at week-4 lead time (13–19 January 2023 valid period), but with relatively low confidence, and with considerable uncertainty in the ECCC ensemble.

CW3E has regularly produced these experimental subseasonal synthesis forecast products on its website during winter 2022/23 (cw3e.ucsd.edu/s2s_forecasts). The case study presented here for the 22 December 2022 forecast shows an example of the potential utility of these experimental subseasonal synthesis forecast products in conveying information in a concise graphical way that helps end users understand how odds are titled toward wet or dry conditions in the coming weeks across California and the Pacific Northwest.

Summary and future directions

In this work, observations and experimental subseasonal and seasonal forecasts from the unusually wet winter of 2022/23 were examined in detail over California and the upper Colorado River basin (seasonal only). Due largely to a family of nine landfalling

atmospheric rivers (ARs) over California in late December 2022 and early January 2023, the intense multiyear drought that plagued California and much of the western United States was substantially alleviated (except over extreme Northern California and parts of the Mojave Desert), with reservoirs generally replenished and massive snowpack accumulated across the region by the arrival of spring. We note that despite this relief in the form of heavy and continuous precipitation, wetlands and forests across the western United States still bear the scars of the extensive drought, and groundwater overdrafts remain unreplenished. The Colorado River basin storage in Lakes Powell and Mead also remains very low, and these reservoirs would require multiple years of well above-normal precipitation to fully recover from the drought since they can hold up to 4 years of normal runoff. This highlights the cumulative impacts of the extreme drought that will persist beyond this winter. In addition, devastating flooding and debris flows across California caused by landfalling ARs and their associated extreme precipitation were widespread, highlighting the hazardous counterparts associated with the beneficial relief that the state experienced. It is also noteworthy that although the December 2022–January 2023 period was critical in alleviating multiyear drought conditions over California, much of the state continued to receive steady precipitation and accumulated snowpack during the rest of the winter and through early spring, which was important as well (e.g., Fig. 2).

New experimental seasonal and subseasonal synthesis forecast products created at CW3E (2023) in collaboration with several universities, institutions, and agencies (for contributors, see Figs. 6 and 12), along with California Department of Water Resources (DWR) stakeholders, were also introduced in the context of experimental forecasts made during this winter (Figs. 6 and 12). These products are designed to provide concise situational awareness guidance to western U.S. water managers and other applied end users based on relevant experimental seasonal and subseasonal forecast products for this region.

Nearly all the experimental seasonal forecasts of wintertime precipitation anomalies over the western United States, made in late autumn 2022, incorrectly predicted drier-than-normal conditions over Southern California. Although dryness was observed over the interior deserts, the heavily populated coastal Southern California region was much wetter than normal. Experimental seasonal forecasts over Northern California were dominated by the uncertain/equal-chances or normal categories (four and two predictions, respectively), whereas observed precipitation anomalies were broadly above normal during this period. Over the upper Colorado basin, there was also considerable uncertainty across the different experimental seasonal forecasts, with at least two experimental predictions favoring each of the normal, above-normal, and uncertain/equal-chances categories (three, two, and two predictions, respectively). Observed precipitation anomalies during the November 2022–January 2023 period were above normal in this region. Several prediction systems made particularly accurate forecasts of above-normal precipitation across the western U.S. region, including the CW3E XGBoost and neural network machine learning models, as well as the NMME GFDL-SPEAR model. However, it is possible these accurate predictions for only one season occurred by chance. Future studies focused on which sources of predictability were useful in these prediction systems for the winter 2022/23 forecast would be very valuable.

Ongoing and future research on experimental seasonal prediction holds promise for improvements over current levels of skill. Merging forecast information on subseasonal time scales into seasonal prediction systems is an area of active research and has also been explored in previous studies (e.g., Yang et al. 2018). It is also noteworthy that when applying CW3E's experimental seasonal prediction system based on CCA analysis (Gershunov and Cayan 2003) separately to AR and non-AR precipitation (not shown), skill arises predominantly from predicting seasonal non-AR precipitation, while AR precipitation skill is low to the point of

degrading the total seasonal precipitation forecasting skill. This suggests a key role for ARs as disruptors to skillful experimental seasonal precipitation forecasts and indicates that future research should focus on revising and refining some of the approaches to experimental seasonal forecasting discussed in this work. Additionally, process studies investigating physical drivers in the climate system beyond ENSO that may increase the likelihood of disruptive ARs impacting California should be undertaken.

Observed diagnostics of the circulation regime shift that occurred across the North Pacific and western U.S. region in late December and early January 2023 were investigated in this study, along with a concurrent MJO transition from phases 4 and 5 to phases 6 and 7 that is consistent with an increased likelihood of extreme precipitation and AR activity over California. However, the persistence of the AR activity along the California coastline during this period was unusually intense and unlikely to be explained by the MJO transition alone. We note that based on the results from Castellano et al. (2023), the likelihood of wet conditions during NDJ under westerly QBO conditions, which were observed during the period of interest last winter, generally decreases over California. During JFM, very few combinations of MJO phase and lag time result in significantly increased probabilities of wet conditions under westerly QBO conditions. Therefore, based on these findings, the role of the QBO as a physical driver behind the observed regime shift from dry to wet over California in late December 2022 is unclear.

A closer examination of experimental subseasonal circulation regime and AR activity forecasts during late December 2022 and early January 2023 was provided. In general, the dynamical model ensembles, which provide data for the experimental subseasonal forecast products discussed in this study, were able to capture broad signals of a regime shift from ridging/dry to troughing/wet conditions at weeks-2–3 lead time over the North Pacific and western United States, as well as the temporary return to dry conditions and below-normal AR activity during the 20–26 January 2023 period (Figs. 10 and 11). Despite this compelling case study, subseasonal predictability of AR activity, regime shifts, and precipitation swings over California remains a challenging endeavor, and dynamical ensembles will not always capture future analogous swings in regional climate. Future studies further examining the underlying dynamical evolution of this remarkable 3 week period over the North Pacific and western U.S. region, with an eye toward linkages to subseasonal predictability in dynamical models, would thus be highly valuable.

A new CW3E experimental subseasonal synthesis forecast product was shown for the 0000 UTC 22 December 2022 multimodel dynamical ensemble forecasts (Fig. 12), and its process of development with stakeholders at the California DWR was described in detail. These experimental subseasonal synthesis products were regularly included in CW3E outlooks during winter 2022/23 and will be routinely provided to end users in subsequent winters.

International collaboration and scientific innovations have helped improve the fidelity of experimental seasonal and subseasonal prediction systems over the last decade, which has been demonstrated by the development of new prediction systems with skill comparable to or exceeding that of existing methods (e.g., Gibson et al. 2021; Switanek and Hamill 2022; and others). However, fundamental challenges remain to provide useful information for stakeholders at these extended lead times. This is especially true for the problem of seasonal prediction, which is far more constrained by sampling variability over the historical record compared to experimental subseasonal predictions. However, with continued investment across the international research community, forecast improvements can likely be achieved. There is still substantial room for innovations both in science topics (e.g., the generation of high-resolution dynamical hindcast ensemble systems and the training of new machine learning methods on relevant observations and model data) and the process of collaboration between researchers and stakeholders analogous to the examples described here. The analysis in this study of the

important winter 2022/23 regime shift that brought much needed drought relief to California explores both the promise and some limitations of the diverse array of recently developed experimental subseasonal and seasonal prediction tools at CW3E and collaborating institutions.

Data availability statement. Hindcast data used to calculate model climatologies used in this study are available as part of the S2S database (https://apps.ecmwf.int/datasets/data/s2s/levtype=sfc/type=cf/). Real-time NCEP CFSv2 data are available via CPC (www.nco.ncep.noaa.gov/pmb/products/cfs/); the real-time ECMWF and ECCC data used in this study were obtained as part of a research license agreement with each institution. Observational data used in this study are publicly available and include U.S. Drought Monitor forecasts (https://droughtmonitor.unl.edu/Data.aspx), precipitation data from the California Data Exchange Center (2023) (https://cdec.water.ca.gov/snow_rain.html), the SIO-R1 AR catalog (https://weclima.ucsd.edu/data-products/), PRISM (https://prism.oregonstate.edu), version 5 of the ECMWF reanalysis (ERA5; www.ecmwf.int/en/forecasts/dataset/ecmwf-reanalysis-v5), and the Guan and Waliser AR Detection Algorithm version 3 (https://dataverse.ucla.edu/dataset.xhtml?persistentId=doi:10.25346/S6/YO15ON).

References

Becker, E. J., B. P. Kirtman, M. L'Heureux, Á. G. Muñoz, and K. Pegion, 2022: A decade of the North American Multimodel Ensemble (NMME): Research, application, and future directions. *Bull. Amer. Meteor. Soc.*, **103**, E973–E995, https://doi.org/10.1175/BAMS-D-20-0327.1.

California Data Exchange Center, 2023: Tulare basin precipitation: 6-station index, December 12, 2023. CDEC Rep., 1 p., https://cdec.water.ca.gov/cgi-progs/products/PLOT_TSI.pdf.

Castellano, C. M., and Coauthors, 2023: Development of a statistical subseasonal forecast tool to predict California atmospheric rivers and precipitation based on MJO and QBO activity. *J. Geophys. Res. Atmos.*, **128**, e2022JD037360, https://doi.org/10.1029/2022JD037360.

Chapman, W. E., A. C. Subramanian, S. Xie, M. D. Sierks, F. M. Ralph, and Y. Kamae, 2021: Monthly modulations of ENSO teleconnections: Implications for potential predictability in North America. *J. Climate*, **34**, 5899–5921, https://doi.org/10.1175/JCLI-D-20-0391.1.

CW3E, 2023: Subseasonal to seasonal forecasts. Accessed 30 April 2023, https://cw3e.ucsd.edu/s2s_forecasts/.

Daly, C., M. Halbleib, J. I. Smith, W. P. Gibson, M. K. Doggett, G. H. Taylor, J. Curtis, and P. P. Pasteris, 2008: Physiographically sensitive mapping of climatological temperature and precipitation across the conterminous United States. *Int. J. Climatol.*, **28**, 2031–2064, https://doi.org/10.1002/joc.1688.

DeFlorio, M. J., D. W. Pierce, D. R. Cayan, and A. J. Miller, 2013: Western U.S. extreme precipitation events and their relation to ENSO and PDO in CCSM4. *J. Climate*, **26**, 4231–4243, https://doi.org/10.1175/JCLI-D-12-00257.1.

——, D. E. Waliser, B. Guan, F. M. Ralph, and F. Vitart, 2019a: Global evaluation of atmospheric river subseasonal prediction skill. *Climate Dyn.*, **52**, 3039–3060, https://doi.org/10.1007/s00382-018-4309-x.

——, and Coauthors, 2019b: Experimental subseasonal-to-seasonal (S2S) forecasting of atmospheric rivers over the western United States. *J. Geophys. Res. Atmos.*, **124**, 11242–11265, https://doi.org/10.1029/2019JD031200.

——, F. M. Ralph, D. E. Waliser, J. Jones, and M. L. Anderson, 2021: Better subseasonal-to-seasonal forecasts for water management. *Eos*, **102**, https://doi.org/10.1029/2021EO159749.

Deng, Y., and T. Jiang, 2011: Intraseasonal modulation of the North Pacific storm track by tropical convection in boreal winter. *J. Climate*, **24**, 1122–1137, https://doi.org/10.1175/2010JCLI3676.1.

Dettinger, M. D., 2013: Atmospheric rivers as drought busters on the U.S. West Coast. *J. Hydrometeor.*, **14**, 1721–1732, https://doi.org/10.1175/JHM-D-13-02.1.

——, F. M. Ralph, T. Das, P. J. Neiman, and D. R. Cayan, 2011: Atmospheric rivers, floods and the water resources of California. *Water*, **3**, 445–478, https://doi.org/10.3390/w3020445.

Fang, X., and Coauthors, 2023: Will the historic southeasterly wind over the equatorial Pacific in March 2022 trigger a third-year La Niña event? *Adv. Atmos. Sci.*, **40**, 6–13, https://doi.org/10.1007/s00376-022-2147-6.

Fish, M. A., A. M. Wilson, and F. M. Ralph, 2019: Atmospheric river families: Definition and associated synoptic conditions. *J. Hydrometeor.*, **20**, 2091–2108, https://doi.org/10.1175/JHM-D-18-0217.1.

Gershunov, A., and D. Cayan, 2003: Heavy daily precipitation frequency over the contiguous United States: Sources of climatic variability and seasonal predictability. *J. Climate*, **16**, 2752–2765, https://doi.org/10.1175/1520-0442(2003)016<2752:HDPFOT>2.0.CO;2.

——, T. Shulgina, F. M. Ralph, D. A. Lavers, and J. J. Rutz, 2017: Assessing the climate-scale variability of atmospheric rivers affecting western North America. *Geophys. Res. Lett.*, **44**, 7900–7908, https://doi.org/10.1002/2017GL074175.

Gibson, P. B., D. E. Waliser, B. Guan, M. J. DeFlorio, F. M. Ralph, and D. L. Swain, 2020a: Ridging associated with drought in the western and southwestern United States: Characteristics, trends, and predictability sources. *J. Climate*, **33**, 2485–2508, https://doi.org/10.1175/JCLI-D-19-0439.1.

——, ——, A. Goodman, M. J. DeFlorio, L. Delle Monache, and A. Molod, 2020b: Subseasonal-to-seasonal hindcast skill assessment of ridging events related to drought over the western United States. *J. Geophys. Res. Atmos.*, **125**, e2020JD033655, https://doi.org/10.1029/2020JD033655.

——, W. E. Chapman, A. Altinok, L. Delle Monache, M. J. DeFlorio, and D. E. Waliser, 2021: Training machine learning models on climate model output yields skillful interpretable seasonal precipitation forecasts. *Nat. Commun. Earth Environ.*, **2**, 159, https://doi.org/10.1038/s43247-021-00225-4.

Gottschalck, J., and Coauthors, 2010: A framework for assessing operational Madden–Julian oscillation forecasts: A CLIVAR MJO Working Group project. *Bull. Amer. Meteor. Soc.*, **91**, 1247–1258, https://doi.org/10.1175/2010BAMS2816.1.

Guan, B., and D. E. Waliser, 2015: Detection of atmospheric rivers: Evaluation and application of an algorithm for global studies. *J. Geophys. Res. Atmos.*, **120**, 12514–12535, https://doi.org/10.1002/2015JD024257.

——, ——, N. P. Molotch, E. J. Fetzer, and P. J. Neiman, 2012: Does the Madden–Julian oscillation influence wintertime atmospheric rivers and snowpack in the Sierra Nevada? *Mon. Wea. Rev.*, **140**, 325–342, https://doi.org/10.1175/MWR-D-11-00087.1.

——, ——, and F. M. Ralph, 2018: An intercomparison between reanalysis and dropsonde observations of the total water vapor transport in individual atmospheric rivers. *J. Hydrometeor.*, **19**, 321–337, https://doi.org/10.1175/JHM-D-17-0114.1.

Guirguis, K., A. Gershunov, M. J. DeFlorio, T. Shulgina, L. Delle Monache, A. C. Subramanian, T. W. Corringham, and F. M. Ralph, 2020: Four atmospheric circulation regimes over the North Pacific and their relationship to California precipitation on daily to seasonal timescales. *Geophys. Res. Lett.*, **47**, e2020GL087609, https://doi.org/10.1029/2020GL087609.

——, and Coauthors, 2022: Winter wet–dry weather patterns driving atmospheric rivers and Santa Ana winds provide evidence for increasing wildfire hazard in California. *Climate Dyn.*, **60**, 1729–1749, https://doi.org/10.1007/s00382-022-06361-7.

Hersbach, H., and Coauthors, 2020: The ERA5 global reanalysis. *Quart. J. Roy. Meteor. Soc.*, **146**, 1999–2049, https://doi.org/10.1002/qj.3803.

IRI, 2023: Seasonal climate forecast. Accessed 23 April 2023, https://iri.columbia.edu/our-expertise/climate/forecasts/seasonal-climate-forecasts/.

Jiang, X., D. E. Waliser, P. B. Gibson, G. Chen, and W. Guan, 2022: Why seasonal prediction of California winter precipitation is challenging. *Bull. Amer. Meteor. Soc.*, **103**, E2688–E2700, https://doi.org/10.1175/BAMS-D-21-0252.1.

Kirtman, B. P., and Coauthors, 2014: The North American Multimodel Ensemble: Phase-1 seasonal-to-interannual prediction; phase-2 toward developing intraseasonal prediction. *Bull. Amer. Meteor. Soc.*, **95**, 585–601, https://doi.org/10.1175/BAMS-D-12-00050.1.

Krishnakumar, P., and S. Kannan, 2020: The worst fire season ever. Again. *Los Angeles Times*, 15 September, www.latimes.com/projects/california-fires-damage-climate-change-analysis.

Madden, R. A., and P. R. Julian, 1971: Detection of a 40–50 day oscillation in the zonal wind in the tropical Pacific. *J. Atmos. Sci.*, **28**, 702–708, https://doi.org/10.1175/1520-0469(1971)028<0702:DOADOI>2.0.CO;2.

——, and ——, 1972: Description of a global-scale circulation cells in the tropics with a 40–50 day period. *J. Atmos. Sci.*, **29**, 1109–1123, https://doi.org/10.1175/1520-0469(1972)029<1109:DOGSCC>2.0.CO;2.

Mariotti, A., and Coauthors, 2020: Windows of opportunity for skillful forecasts subseasonal to seasonal and beyond. *Bull. Amer. Meteor. Soc.*, **101**, E608–E625, https://doi.org/10.1175/BAMS-D-18-0326.1.

Matza, M., 2023: Evacuations ordered in California as deadly storm slams into coast. BBC News, accessed 12 April 2023, www.bbc.com/news/world-us-canada-64169954.

Merryfield, W. J., and Coauthors, 2020: Current and emerging developments in subseasonal to decadal prediction. *Bull. Amer. Meteor. Soc.*, **101**, E869–E896, https://doi.org/10.1175/BAMS-D-19-0037.1.

Moody's RMS, 2023: Moody's RMS estimates US$5-7 billion in total U.S. economic losses from California Flooding. Moody's RMS, accessed 28 April 2023,

www.rms.com/newsroom/press-releases/press-detail/2023-01-25/moodys-rms-estimates-us5-7-billion-in-total-us-economic-losses-from-california-flooding.

Mundhenk, B. D., E. A. Barnes, and E. D. Maloney, 2016: All-season climatology and variability of atmospheric river frequencies over the North Pacific. *J. Climate*, **29**, 4885–4903, https://doi.org/10.1175/JCLI-D-15-0655.1.

——, ——, ——, and C. F. Baggett, 2018: Skillful empirical subseasonal prediction of landfalling atmospheric river activity using the Madden–Julian oscillation and quasi-biennial oscillation. *npj Climate Atmos. Sci.*, **1**, 20177, https://doi.org/10.1038/s41612-017-0008-2.

NASEM, 2010: *Assessment of Intraseasonal to Interannual Climate Prediction and Predictability.* National Academies Press, 192 pp.

——, 2016: *Next Generation Earth System Prediction: Strategies for Subseasonal to Seasonal Forecasts.* National Academies Press, 335 pp.

Ralph, F. M., P. J. Neiman, and G. A. Wick, 2004: Satellite and CALJET aircraft observations of atmospheric rivers over the eastern North Pacific Ocean during the winter of 1997/98. *Mon. Wea. Rev.*, **132**, 1721–1745, https://doi.org/10.1175/1520-0493(2004)132<1721:SACAOO>2.0.CO;2.

——, M. D. Dettinger, M. M. Cairns, T. J. Galarneau, and J. Eylander, 2018: Defining "atmospheric river": How the Glossary of Meteorology helped resolve a debate. *Bull. Amer. Meteor. Soc.*, **99**, 837–839, https://doi.org/10.1175/BAMS-D-17-0157.1.

——, J. J. Rutz, J. M. Cordeira, M. Dettinger, M. Anderson, D. Reynolds, L. J. Schick, and C. Smallcomb, 2019: A scale to characterize the strength and impacts of atmospheric rivers. *Bull. Amer. Meteor. Soc.*, **100**, 269–289, https://doi.org/10.1175/BAMS-D-18-0023.1.

Robertson, A. W., N. Vigaud, J. Yuan, and M. K. Tippett, 2020: Toward identifying subseasonal forecasts of opportunity using North American weather regimes. *Mon. Wea. Rev.*, **148**, 1861–1875, https://doi.org/10.1175/MWR-D-19-0285.1.

Scheftic, W. D., X. Zheng, and M. A. Brunke, 2023: Seasonal forecasting of precipitation, temperature, and snow mass over the western United States by combining ensemble postprocessing with empirical ocean–atmosphere teleconnections. *Wea. Forecasting*, **38**, 1413–1427, https://doi.org/10.1175/WAF-D-22-0099.1.

Sengupta, A., B. Singh, M. J. DeFlorio, C. Raymond, A. W. Robertson, X. Zeng, D. E. Waliser, and J. Jones, 2022: Advances in subseasonal to seasonal prediction relevant to water management in the western United States. *Bull. Amer. Meteor. Soc.*, **103**, E2168–E2175, https://doi.org/10.1175/BAMS-D-22-0146.1.

Siler, N., Y. Kosaka, S. Xie, and X. Li, 2017: Tropical ocean contributions to California's surprisingly dry El Niño of 2015/16. *J. Climate*, **30**, 10067–10079, https://doi.org/10.1175/JCLI-D-17-0177.1.

Singh, D., M. Ting, A. A. Scaife, and N. Martin, 2018: California winter precipitation predictability: Insights from the anomalous 2015–2016 and 2016–2017

seasons. *Geophys. Res. Lett.*, **45**, 9972–9980, https://doi.org/10.1029/2018GL078844.

Switanek, M. B., and T. M. Hamill, 2022: A new methodology to produce more skillful United States cool-season precipitation forecasts. *J. Hydrometeor.*, **23**, 991–1005, https://doi.org/10.1175/JHM-D-21-0235.1.

Toohey, G., and S. Rust, 2023: Massive "atmospheric river" to bring heavy rains, winds, flooding across California. *Los Angeles Times*, 3 January, www.latimes.com/california/story/2023-01-03/another-atmospheric-river-expected-for-california.

Toride, K., and G. J. Hakim, 2022: What distinguishes MJO events associated with atmospheric rivers? *J. Climate*, **35**, 6135–6149, https://doi.org/10.1175/JCLI-D-21-0493.1.

Vitart, F., and Coauthors, 2017: The Subseasonal to Seasonal (S2S) Prediction project database. *Bull. Amer. Meteor. Soc.*, **98**, 163–173, https://doi.org/10.1175/BAMS-D-16-0017.1.

Waliser, D. E., and Coauthors, 2006: The Experimental MJO Prediction Project. *Bull. Amer. Meteor. Soc.*, **87**, 425–431, https://doi.org/10.1175/BAMS-87-4-421.

Wang, J., M. J. DeFlorio, B. Guan, and C. M. Castellano, 2023: Seasonality of MJO impacts on precipitation extremes over the western United States. *J. Hydrometeor.*, **24**, 151–166, https://doi.org/10.1175/JHM-D-22-0089.1.

White, C. J., and Coauthors, 2022: Advances in the application and utility of subseasonal-to-seasonal predictions. *Bull. Amer. Meteor. Soc.*, **103**, E1448–E1472, https://doi.org/10.1175/BAMS-D-20-0224.1.

Xie, P., M. Chen, S. Yang, A. Yatagai, T. Hayasaka, Y. Fukushima, and C. Liu, 2007: A gauge-based analysis of daily precipitation over East Asia. *J. Hydrometeor.*, **8**, 607–626, https://doi.org/10.1175/JHM583.1.

Yang, X., L. Jia, S. B. Kapnick, T. L. Delworth, G. A. Vecchi, R. Gudgel, S. Underwood, and F. Zeng, 2018: On the seasonal prediction of the western United States El Niño precipitation pattern during the 2015/16 winter. *Climate Dyn.*, **51**, 3765–3783, https://doi.org/10.1007/s00382-018-4109-3.

Zhang, Z., and Coauthors, 2023: Multi-model subseasonal prediction skill assessment of water vapor transport associated with atmospheric rivers over the western U.S. *J. Geophys. Res. Atmos.*, **128**, e2022JD037608, https://doi.org/10.1029/2022JD037608.

Zhou, S., M. L'Heureux, S. Weaver, and A. Kumar, 2012: A composite study of the MJO influence on the surface air temperature and precipitation over the continental United States. *Climate Dyn.*, **38**, 1459–1471, https://doi.org/10.1007/s00382-011-1001-9.

Zhou, Y., H. Kim, and D. E. Waliser, 2021: Atmospheric river lifecycle responses to the Madden-Julian oscillation. *Geophys. Res. Lett.*, **48**, e2020GL090983, https://doi.org/10.1029/2020GL090983.

Zhu, Y., and R. E. Newell, 1998: A proposed algorithm for moisture fluxes from atmospheric rivers. *Mon. Wea. Rev.*, **126**, 725–735, https://doi.org/10.1175/1520-0493(1998)126<0725:APAFMF>2.0.CO;2.